2D carboxylate-bridged Ln^{III} coordination polymers: displaying the slow magnetic relaxation and luminescent properties in detection of Fe^{3+}, $Cr_2O_7^{2-}$ and nitrobenzene

Wei Gao[ab], Feng Liu[b], Bao-Ying Zhang[a], Xiu-Mei Zhang[bc], Jie-Ping Liu[b], En-Qing Gao[d] and Qing-Yu Gao*[a]*

Table S1 Selected bond lengths (Å) and angles (°) for **1-Nd**

Nd1-O4A	2.323(2)	Nd1-O2B	2.349(2)
Nd1-O3C	2.372(2)	Nd1-O1	2.389(2)
Nd1-O9	2.502(2)	Nd1-O6	2.512(2)
Nd1-O7	2.560(3)	Nd1-O8	2.563(2)
O4A-Nd1-O3C	98.78(7)	O2B-Nd1-O3C	85.73(7)
O4A-Nd1-O1	83.78(7)	O2B-Nd1-O1	100.49(8)
O3C-Nd1-O1	148.83(8)	O4A-Nd1-O9	74.10(8)
O2B-Nd1-O9	92.77(9)	O3C-Nd1-O9	71.51(8)
O1-Nd1-O9	137.66(8)	O4A-Nd1-O6	85.06(8)
O2B-Nd1-O6	81.50(8)	O3C-Nd1-O6	139.58(8)
O1-Nd1-O6	71.50(7)	O9-Nd1-O6	71.01(8)
O4A-Nd1-O7	123.51(9)	O2B-Nd1-O7	72.72(9)
O3C-Nd1-O7	76.78(8)	O1-Nd1-O7	76.07(8)
O9-Nd1-O7	146.02(8)	O6-Nd1-O7	133.61(8)
O4A-Nd1-O8	74.39(8)	O2B-Nd1-O8	121.85(9)
O3C-Nd1-O8	74.58(8)	O1-Nd1-O8	76.31(7)
O9-Nd1-O8	128.70(8)	O6-Nd1-O8	143.37(8)
O7-Nd1-O8	49.82(8)	O4A-Nd1-O2B	163.72(9)

Symmetry codes: A :-x-1, -y-1, -z-1; B:-x-1, y+1/2, -z-3/2; C:x, y+1, z

Table S2 Selected bond lengths (Å) and angles (°) for **1-Sm**

Sm1-O4A	2.292(2)	Sm1-O2B	2.317(2)
Sm1- O3C	2.344(2)	Sm1-O1	2.363(2)
Sm1-O9	2.470(3)	Sm1-O6	2.478(3)
Sm1-O7	2.533(3)	Sm1-O8	2.541(3)
O4A-Sm1-O3C	98.34(9)	O2B-Sm1-O3C	85.93(9)
O4A-Sm1-O1	84.08(9)	O2B-Sm1-O1	100.81(9)
O3C-Sm1-O1	148.67(9)	O4A-Sm1-O9	74.69(10)
O2B-Sm1-O9	91.43(11)	O3C-Sm1-O9	70.80(10)
O1-Sm1-O9	138.26(9)	O4A-Sm1-O6	84.76(9)
O2B-Sm1-O6	81.50(10)	O3C-Sm1-O6	139.56(9)

O1-Sm1-O6	71.72(9)	O9-Sm1-O6	70.91(9)
O4A-Sm1-O7	124.29(10)	O2B-Sm1-O7	72.61(11)
O3C-Sm1-O7	77.02(10)	O1-Sm1-O7	75.99(9)
O9-Sm1-O7	145.32(10)	O6-Sm1-O7	133.48(10)
O4A-Sm1-O8	74.74(9)	O2B-Sm1-O8	122.10(10)
O3C-Sm1-O8	74.34(9)	O1-Sm1-O8	76.27(8)
O9-Sm1-O8	129.20(9)	O6-Sm1-O8	143.45(9)
O7-Sm1-O8	50.24(10)	O4A-Sm1-O2B	163.07(10)
Symmetry codes: A :-x-1, -y-1, -z-1; B:-x-1, y+1/2, -z-3/2; C:x, y+1, z			

Table S3 Selected bond lengths (Å) and angles (°) for **1-Eu**

Eu1-O4A	2.214(2)	Eu1-O2B	2.238(2)
Eu1-O3C	2.268(2)	Eu1-O1	2.287(2)
Eu1-O9	2.391(3)	Eu1-O6	2.403(2)
Eu1-O7	2.450(3)	Eu1-O8	2.494(3)
O4A-Eu1-O3C	97.46(8)	O2B-Eu1-O3C	86.56(8)
O4A-Eu1-O1	84.77(8)	O2B-Eu1-O1	101.16(9)
O3C-Eu1-O1	148.27(8)	O4A-Eu1-O9	76.18(10)
O2B-Eu1-O9	88.55(11)	O3C-Eu1-O9	70.55(9)
O1-Eu1-O9	139.57(8)	O4A-Eu1-O6	84.32(9)
O2B-Eu1-O6	81.20(9)	O3C-Eu1-O6	139.61(8)
O1-Eu1-O6	72.11(8)	O9-Eu1-O6	70.79(9)
O4A-Eu1-O7	126.09(9)	O2B-Eu1-O7	72.14(10)
O3C-Eu1-O7	77.93(9)	O1-Eu1-O7	75.40(8)
O9-Eu1-O7	143.91(9)	O6-Eu1-O7	132.51(9)
O4A-Eu1-O8	75.32(8)	O2B-Eu1-O8	122.77(9)
O3C-Eu1-O8	73.95(8)	O1-Eu1-O8	76.09(8)
O9-Eu1-O8	130.40(9)	O6-Eu1-O8	143.51(8)
O7-Eu1-O8	51.52(9)	O4A-Eu1-O2B	161.75(10)
Symmetry codes: A :-x-1, -y-1, -z-1; B:-x-1, y+1/2, -z-3/2; C:x, y+1, z			

Table S4 Selected bond lengths (Å) and angles (°) for **1-Gd**

Gd1-O4A	2.273(2)	Gd1-O2B	2.298(2)
Gd1-O3C	2.319(2)	Gd1-O1	2.339(2)
Gd1-O9	2.443(3)	Gd1-O6	2.452(2)
Gd1-O7	2.503(3)	Gd1-O8	2.522(3)
O4A-Gd1-O3C	98.19(9)	O2B-Gd1-O3C	86.17(9)
O4A-Gd1-O1	84.39(8)	O2B-Gd1-O1	100.90(9)
O3C-Gd1-O1	148.46(8)	O4A-Gd1-O9	75.13(10)
O2B-Gd1-O9	90.28(11)	O3C-Gd1-O9	70.92(9)

O1-Gd1-O9	138.86(9)	O4A-Gd1-O6	84.41(9)
O2B-Gd1-O6	81.25(10)	O3C-Gd1-O6	139.57(9)
O1-Gd1-O6	71.93(8)	O9-Gd1-O6	70.88(9)
O4A-Gd1-O7	125.14(10)	O2B-Gd1-O7	72.57(11)
O3C-Gd1-O7	77.19(9)	O1-Gd1-O7	75.81(9)
O9-Gd1-O7	144.69(10)	O6-Gd1-O7	133.24(9)
O4A-Gd1-O8	75.21(9)	O2B-Gd1-O8	122.43(10)
O3C-Gd1-O8	74.18(8)	O1-Gd1-O8	76.19(8)
O9-Gd1-O8	129.64(9)	O(6)-Gd1-O8	143.53(9)
O7-Gd1-O8	50.64(10)	O4A-Gd1-O2B	162.26(10)
Symmetry codes: A :-x-1, -y-1, -z-1; B:-x-1, y+1/2, -z-3/2; C:x, y+1, z			

Table S5 Selected bond lengths (Å) and angles (°) for **1-Tb**

Tb1-O4A	2.270(3)	Tb1-O2B	2.293(3)
Tb1-O3C	2.318(3)	Tb1-O1	2.339(3)
Tb1-O9	2.437(3)	Tb1-O6	2.453(3)
Tb1-O7	2.503(3)	Tb1-O8	2.521(3)
O4A-Tb1-O3C	98.29(9)	O2B-Tb1-O3C	86.09(9)
O4A-Tb1-O1	84.30(9)	O2B-Tb1-O1	100.82(9)
O3C-Tb1-O1	148.69(9)	O4A-Tb1-O9	75.26(10)
O2B-Tb1-O9	90.31(11)	O3C-Tb1-O9	70.87(10)
O1-Tb1-O9	138.72(9)	O4A-Tb1-O6	84.35(10)
O2B-Tb1-O6	81.36(10)	O3C-Tb1-O6	139.42(10)
O1-Tb1-O6	71.85(9)	O9-Tb1-O6	70.77(10)
O4A-Tb1-O7	125.11(10)	O2B-Tb1-O7	72.46(11)
O3C-Tb1-O7	77.26(10)	O1-Tb1-O7	75.92(10)
O9-Tb1-O7	144.69(10)	O6-Tb1-O7	133.29(10)
O4A-Tb1-O8	75.12(10)	O2B-Tb1-O8	122.39(11)
O3C-Tb1-O8	74.33(10)	O1-Tb1-O8	76.29(9)
O9-Tb1-O8	129.71(10)	O6-Tb1-O8	143.50(10)
O7-Tb1-O8	50.70(10)	O4A-Tb1-O2B	162.41(11)
Symmetry codes: A :-x-1, -y-1, -z-1; B:-x-1, y+1/2, -z-3/2; C:x, y+1, z			

Table S6 Selected bond lengths (Å) and angles (°) for **1-Dy**

Dy1-O2A	2.242(2)	Dy1-O4B	2.269(3)
Dy1-O1	2.298(2)	Dy1-O3C	2.317(2)
Dy1-O9	2.417(3)	Dy1-O6	2.428(3)
Dy1-O7	2.477(3)	Dy1-O8	2.511(3)
O2A-Dy1-O1	97.63(9)	O4B-Dy1-O1	86.36(9)
O2A-Dy1-O3C	84.75(9)	O4B-Dy1-O3C	101.07(9)

O1-Dy1-O3C	148.25(9)	O2A-Dy1-O9	75.74(11)
O4B-Dy1-O9	89.24(12)	O1-Dy1-O9	70.74(10)
O3C- Dy1-O9	139.35(10)	O2A-Dy1-O6	84.38(10)
O4B-Dy1-O6	81.36(10)	O1-Dy1-O6	139.64(9)
O3C-Dy1-O6	72.09(9)	O9-Dy1-O6	70.80(10)
O2A-Dy1-O7	125.59(11)	O4B-Dy1-O7	72.36(11)
O1-Dy1-O7	77.48(10)	O3C-Dy1-O7	75.59(9)
O9-Dy1-O7	144.17(11)	O6-Dy1-O7	133.00(10)
O2A-Dy1-O8	75.28(10)	O4B-Dy1-O8	122.53(11)
O1-Dy1-O8	74.00(9)	O3C-Dy1-O8	76.08(9)
O9-Dy1-O8	130.15(11)	O6-Dy1-O8	143.49(9)
O7-Dy1-O8	51.01(11)	O2A- Dy1-O4B	162.04(11)
Symmetry codes: A :-x-1, -y-1, -z-1; B:-x-1, y+1/2, -z-3/2; C:x, y+1, z			

Table S7 Selected bond lengths (Å) and angles (°) for **1-Ho**

Ho1-O4A	2.232(2)	Ho1-O2B	2.259(2)
Ho1-O3C	2.281(2)	Ho1-O1	2.304(2)
Ho1-O9	2.400(3)	Ho1-O6	2.411(3)
Ho1-O7	2.465(3)	Ho1-O8	2.495(3)
O4A-Ho1-O3C	97.46(9)	O2B-Ho1-O3C	86.35(9)
O4A-Ho1-O1	84.86(9)	O2B-Ho1-O1	101.19(9)
O3C-Ho1-O1	148.26(9)	O4A-Ho1-O9	76.05(10)
O2B-Ho1-O9	88.71(11)	O3C-Ho1-O9	70.80(10)
O1-Ho1-O9	139.36(9)	O4A-Ho1-O6	84.41(10)
O2B-Ho1-O6	81.40(10)	O3C-Ho1-O6	139.70(9)
O1-Ho1-O6	72.02(9)	O9-Ho1-O6	70.69(10)
O4A-Ho1-O7	125.98(10)	O2B-Ho1-O7	72.08(11)
O3C-Ho1-O7	77.61(10)	O1-Ho1-O7	75.61(9)
O9-Ho1-O7	143.94(10)	O6-Ho1-O7	132.71(10)
O4A-Ho1-O8	75.22(10)	O2B-Ho1-O8	122.66(10)
O3C-Ho1-O8	74.05(9)	O1-Ho1-O8	76.03(9)
O9-Ho1-O8	130.52(10)	O6-Ho1-O8	143.35(9)
O7-Ho1-O8	51.44(10)	O4A-Ho1-O2B	161.94(11)
Symmetry codes: A :-x-1, -y-1, -z-1; B:-x-1, y+1/2, -z-3/2; C:x, y+1, z			

Table S8 Selected bond lengths (Å) and angles (°) for **1-Yb**

Yb1-O4A	2.1934(18)	Yb1-O2B	2.219(2)
Yb1-O3C	2.2453(18)	Yb1-O1	2.2738(18)
Yb1-O9	2.369(2)	Yb1-O6	2.382(2)
Yb1-O7	2.429(2)	Yb1-O8	2.483(2)

O4A-Yb1-O3C	97.14(7)	O2B-Yb1-O3C	86.81(7)
O4A-Yb1-O1	85.14(7)	O2B-Yb1-O1	101.06(8)
O3C-Yb1-O1	147.90(7)	O4A-Yb1-O9	76.52(9)
O2B-Yb1-O9	87.95(10)	O3C-Yb1-O9	70.70(8)
O1-Yb1-O9	139.90(8)	O4A-Yb1-O6	84.11(8)
O2B-Yb1-O6	81.39(8)	O3C-Yb1-O6	139.94(7)
O1-Yb1-O6	72.16(7)	O9-Yb1-O6	70.74(8)
O4A-Yb1-O7	126.44(8)	O2B-Yb1-O7	71.98(9)
O3C-Yb1-O7	77.86(8)	O1-Yb1-O7	75.25(7)
O9-Yb1-O7	143.50(8)	O6-Yb1-O7	132.49(8)
O4A-Yb1-O8	75.42(8)	O2B-Yb1-O8	122.83(9)
O3C-Yb1-O8	73.73(7)	O1-Yb1-O8	75.95(7)
O9-Yb1-O8	130.83(8)	O6-Yb1-O8	143.27(7)
O7-Yb1-O8	51.74(8)	O4A-Yb1-O2B	161.57(9)

Symmetry codes: A :-x-1, -y-1, -z-1; B:-x-1, y+1/2, -z-3/2; C:x, y+1, z

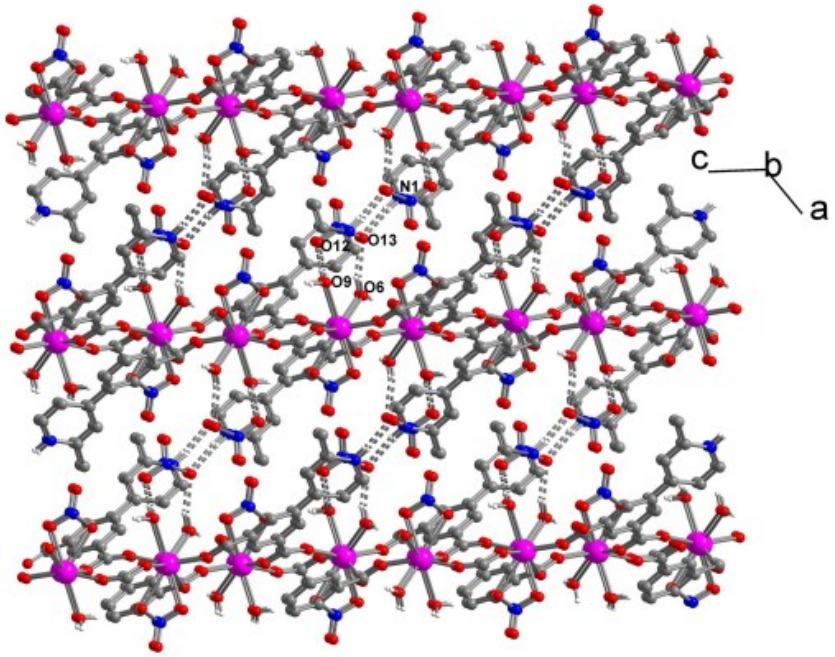

Fig. S1 The 3D packing of the layers in **1-Dy** through hydrogen bonding interactions

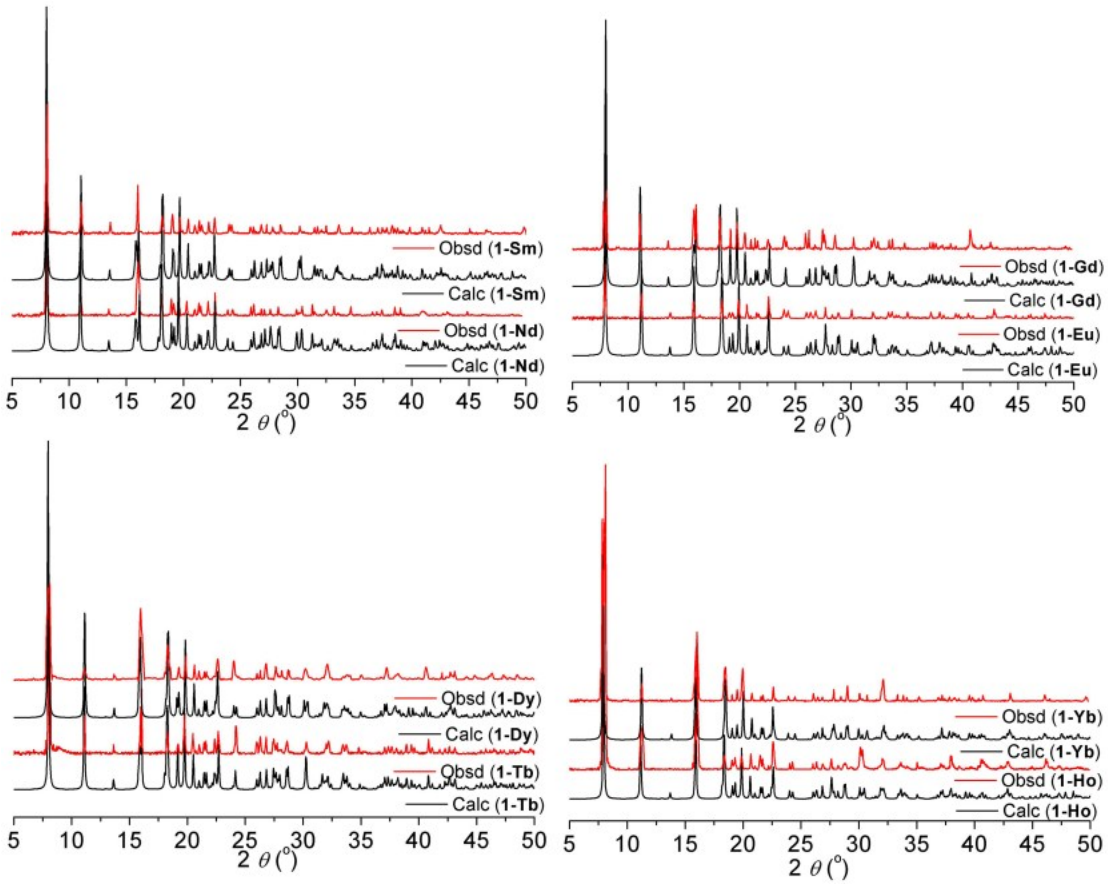

Fig. S2 Powder X-ray diffraction profiles of **1-Nd, 1-Sm, 1-Eu, 1-Gd, 1-Tb, 1-Dy, 1-Ho,** and **1-Yb** together with a simulation from the single crystal data.

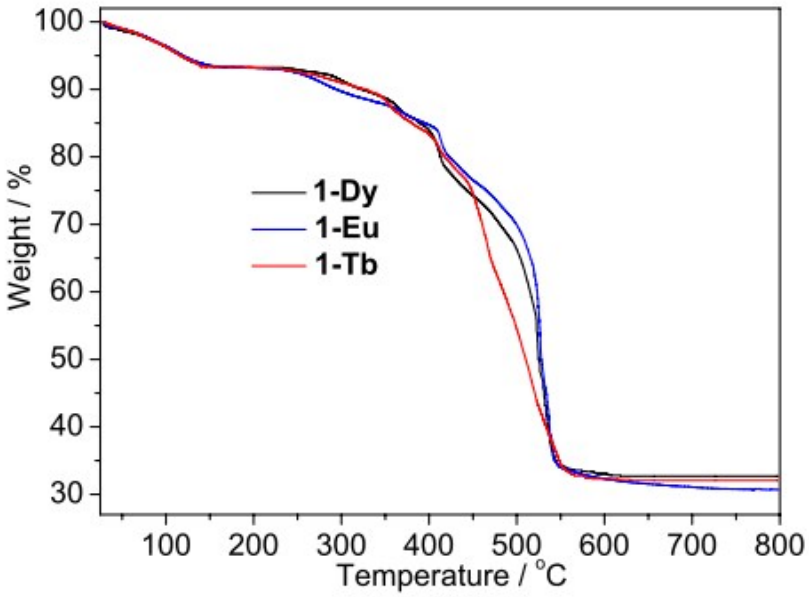

Fig. S3 TG curves of **1-Dy**, **1-Eu** and **1-Tb**.

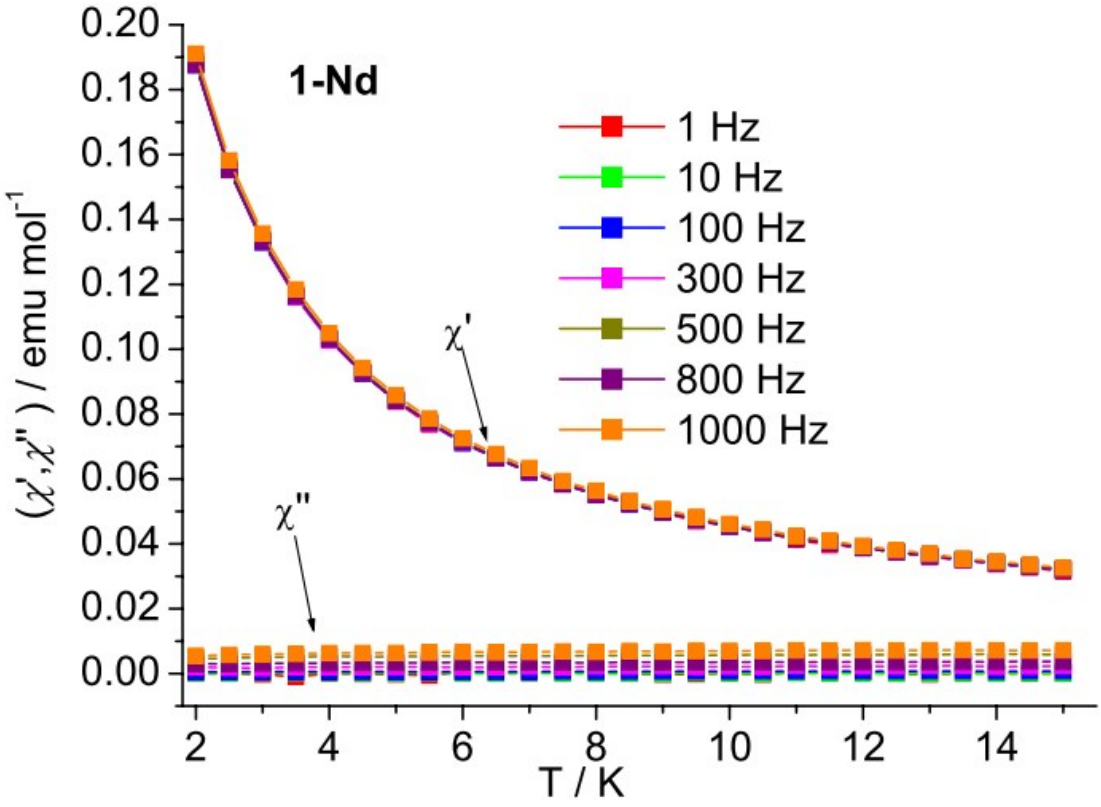

Fig. S4 The ac susceptibilities of **1-Nd** measured at 2 K under H*dc* = 0 elds

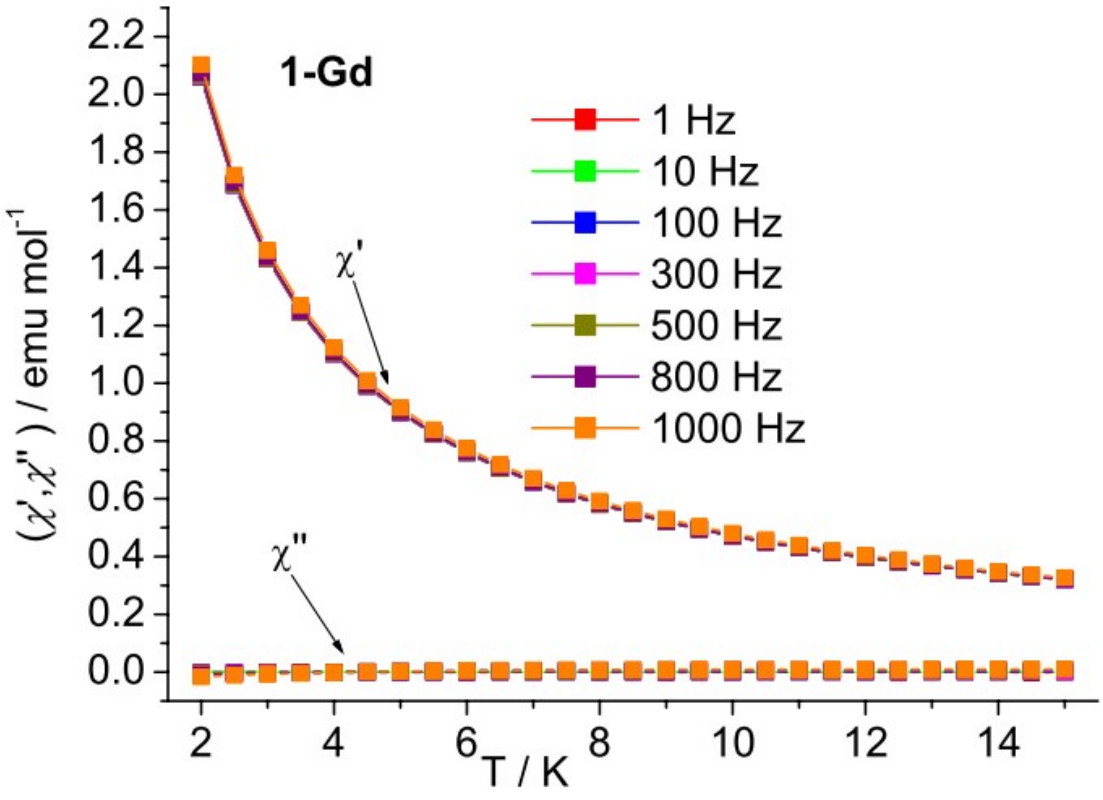

Fig. S5 The ac susceptibilities of **1-Gd** measured at 2 K under H*dc* = 0 elds

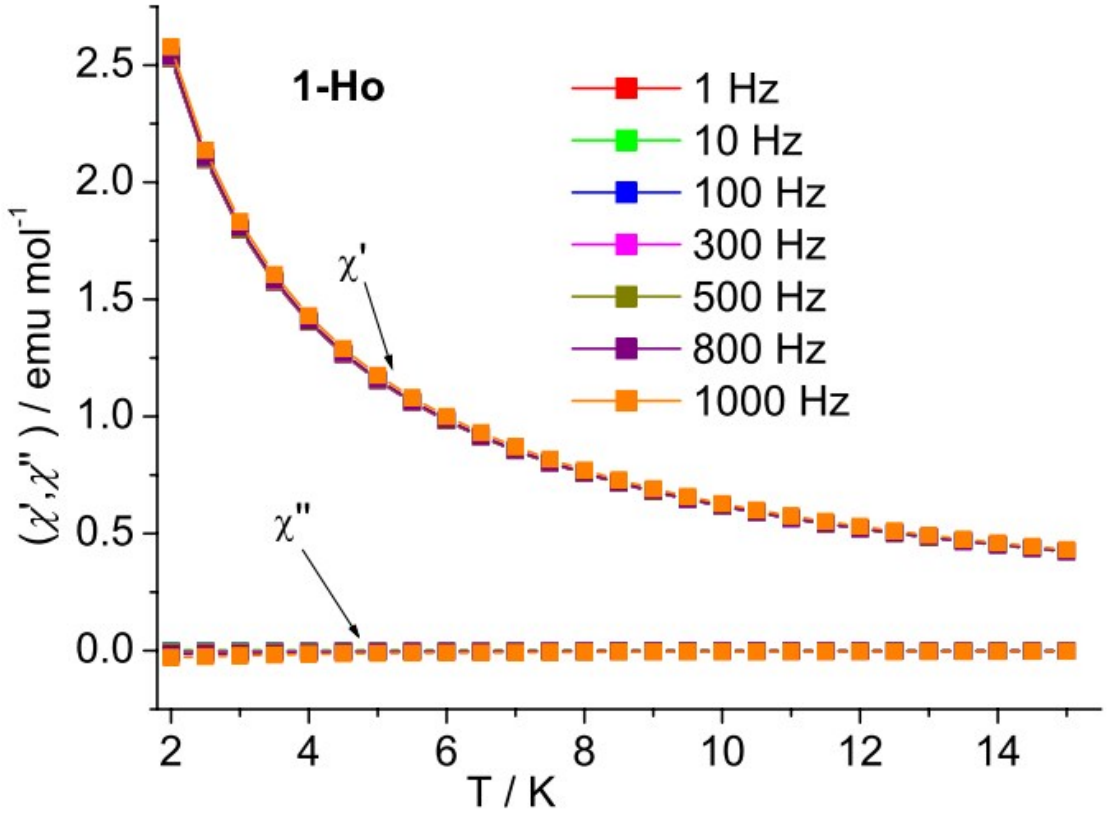

Fig. S6 The ac susceptibilities of **1-Ho** measured at 2 K under H*dc* = 0 elds

Table S9 Relaxation fitting parameters from Least-Squares fitting of □(*f*) data under zero dc field for **1-Dy**.

T (K)	χ_S	χ_T	τ/s	α
5.0	0.159	0.813	0.00379	0.37
6.0	0.146	0.663	0.00268	0.34
7.0	0.138	0.558	0.00191	0.29
8.0	0.131	0.481	0.00129	0.23
9.0	0.125	0.422	0.00073	0.16
10.0	0.115	0.376	0.00033	0.086
11.0	0.0987	0.400	0.00012	0.047

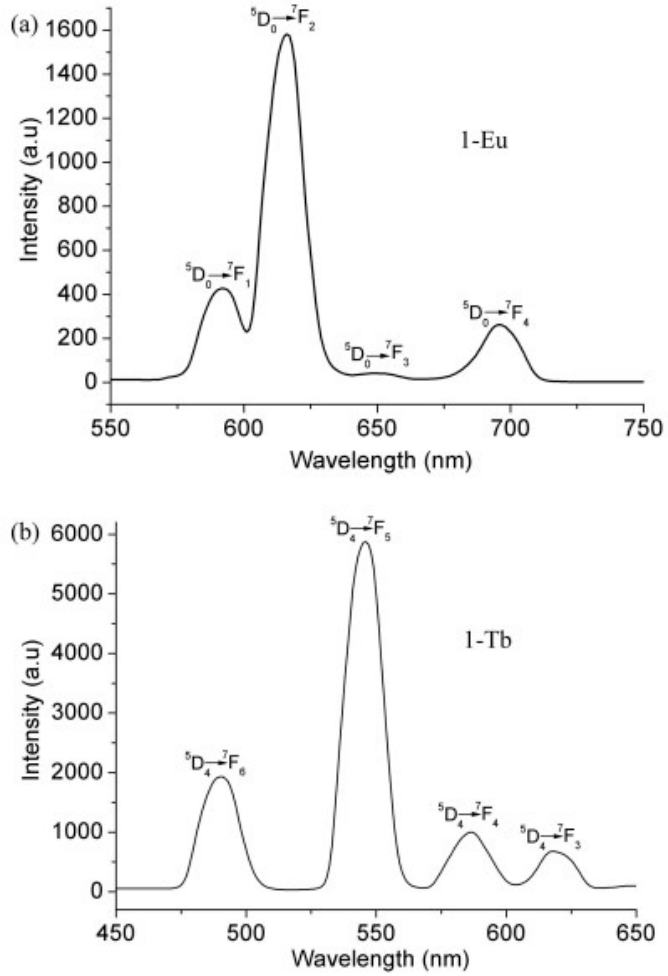

Fig. S7 Solid sample emission spectra of **1-Eu** and **1-Tb** at 298 K.

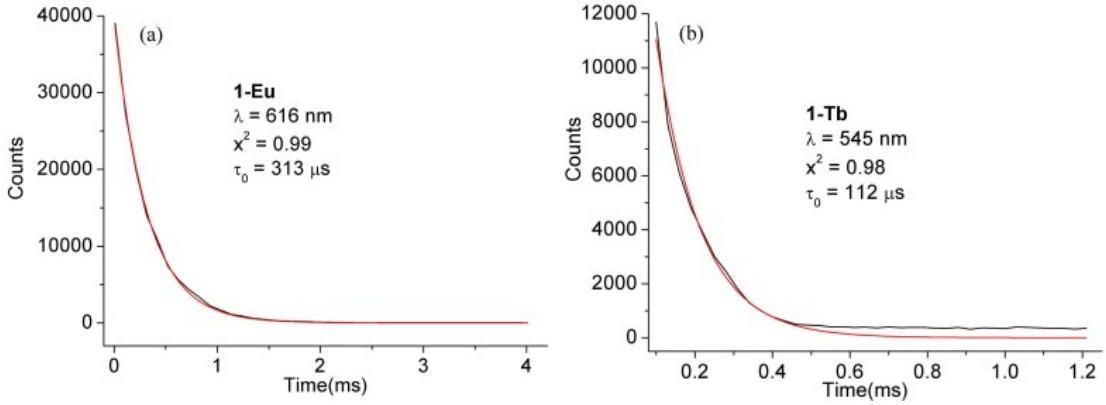

Fig. S8 The fluorescence decay curve for **1-Eu** (a) (λ_{em} = 616 nm) and **1-Tb** (λ_{em} = 545 nm) in solid state at 298 K.

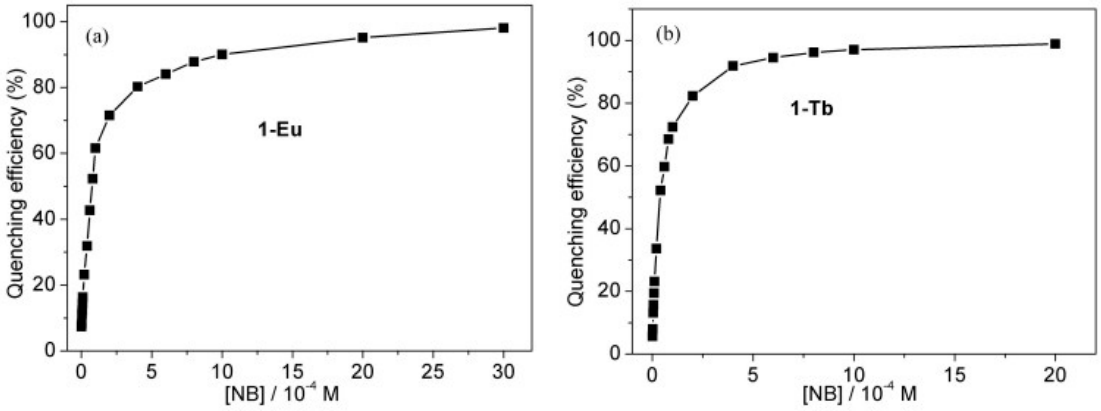

Fig. S9 Quenching efficiency of **1-Eu** (a) and **1-Tb** (b) dispersed in DMF with the addition of NB solution.

Table S10 A comparison between Ln^{III}-based CPs luminescent probes for the detection of nitrobenzene (NB), Fe^{3+} and $Cr_2O_7^{2-}$.

CPs	Analyte	Solution	K_{sv}	Ref.
$[Ln(L_1)(H_2O)_3]\cdot 3H_2O\cdot 0.75DMF$	NB	DMF	------	S1
$\{\{Me_2NH_2\}[Tb^{III}(L_2)]\cdot 3H_2O\cdot DMF\}n$	NB	DMF	4.3×10^2	S2
$[Tb(L_3)_{1.5}(H_2O)](H_2O)_3$	Fe^{3+}	H_2O	------	S3
$[Eu(HL_4)(DMF)(H_2O)_2](H_2O)_3$	Fe^{3+}	H_2O	1.52×10^3	S4
$[Eu(HL_4)(DMF)(H_2O)_2](H_2O)_3$	Fe^{3+}	H_2O	4.48×10^3	S4
$[Eu_2(L_5)_3(DMA)(H_2O)_3](DMA)(H2O)_{4.5}$	Fe^{3+}	H_2O	1.07×10^4	S5
$[H_2NMe_2][Eu(HL_6)]$	Fe^{3+}	H_2O	------	S6
$[Eu(HL_7)_2(NO_3)](H_2O)$	Fe^{3+}	EtOH	------	S7
$[Tb(TBOT)(H_2O)](H_2O)_4(DMF)(NMP)_{0.5}$	Fe^{3+}	H_2O	5.51×10^3	S8
$\{\{Me_2NH_2\}[Tb^{III}(L_2)]\cdot 3H_2O\cdot DMF\}n$	Fe^{3+}	DMF	4.7×10^3	S2
$[Eu(HL_7)_2(NO_3)](H_2O)$	$Cr_2O_7^{2-}$	EtOH	------	S7
$[Tb(TBOT)(H_2O)](H_2O)_4(DMF)(NMP)_{0.5}$	$Cr_2O_7^{2-}$	H_2O	1.37×10^4	S8
$[Eu(L_6)(HCOO)(H_2O)]n$	$Cr_2O_7^{2}$	H_2O	2762.6	S9
$[Tb(L_8)(HCOO)(H_2O)]n$	$Cr_2O_7^{2}$	H_2O	2133.5	S9
$[Ln(L_1)(H_2O)_3]\cdot 3H_2O\cdot 0.75DMF$	$Cr_2O_7^{2}$	H_2O	-------	S1

H_3L_1 = biphenyl-3′-nitro-3,4′,5-tricarboxylic acid;

H_4L_2 = 5-(bis(4-carboxybenzyl)amino)isophthalic acid;

H_2L_3 = 2-(2-hydroxy-propionylamino)-terephthalic acid;

H_4L_4 = 2,8,14,20-tetra-ethyl-6,12,18,24-tetra-methoxy-4,10,16,22-tetra-carboxy-methoxy-calix[4]arene);

H_2L_5 = 9,9-dimethyl-2,7-fluorenedicarboxylic acid;

H_4L_6 = tetrakis[4-(carboxyphenyl)oxamethyl]methane acid;

H_2L_7 = 3-(1H-pyrazol-3-yl) benzoic acid;

H_2L_8 = 5-((2'-cyano-[1,1'-biphenyl]-4-yl)methoxy)isophthalic acid;

H_3TBOT = (2,4,6-tris[1-(3-carboxylphenoxy)ylmethyl]mesitylene);

NMP = N-methyl-2-pyrrolidone;

DMF = dimethylformamide;

DMA = dimethylacetamide.

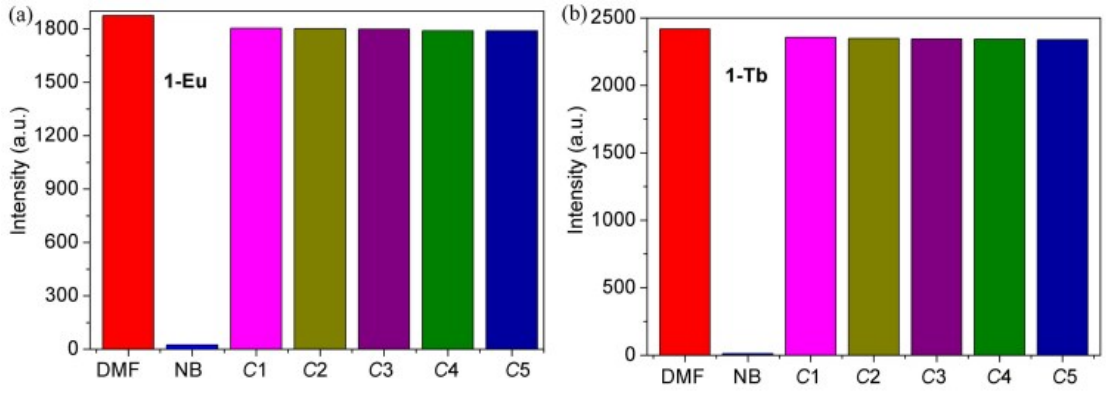

Fig. S10 Luminescence intensity of **1-Eu** (a) and **1-Tb** (b) after five cycles.

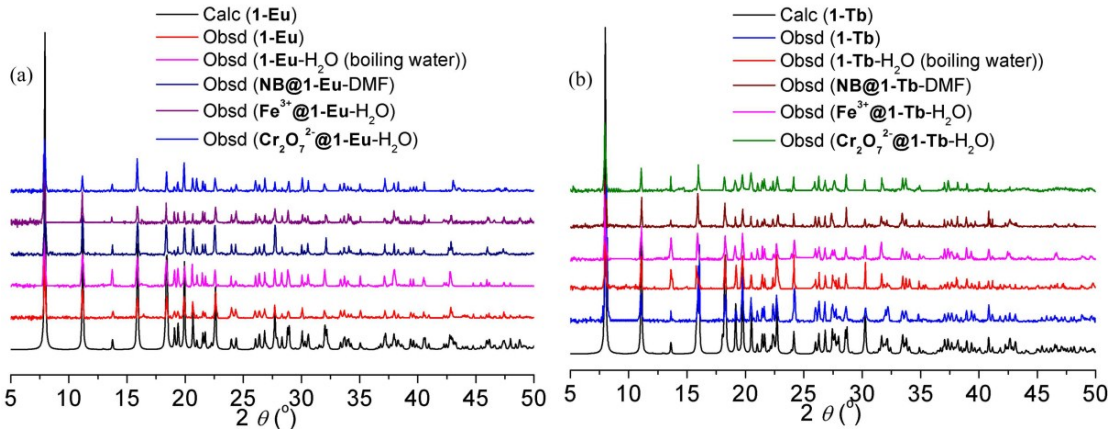

Fig. S11 The PXRD data of the as-synthesized **1-Eu** (a) and **1-Tb** (b) after Fe^{3+}, $Cr_2O_7^{2-}$ and NB sensing process, with the simulated result as reference.

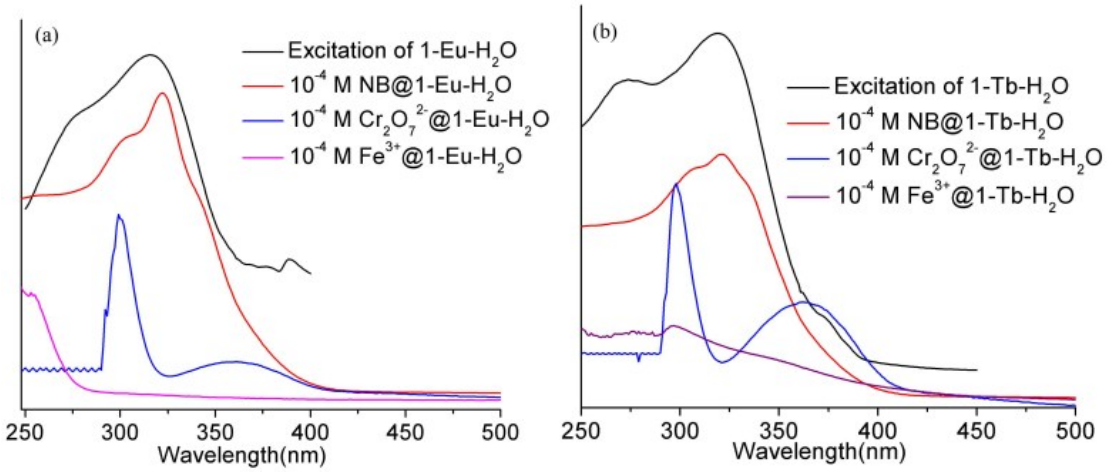

Fig. S12 UV-vis spectra of **1-Eu** (a) and **1-Tb** (b) containing Fe^{3+}, $Cr_2O_7^{2-}$ and NB (1 mM) and corresponding excitation spectrum.

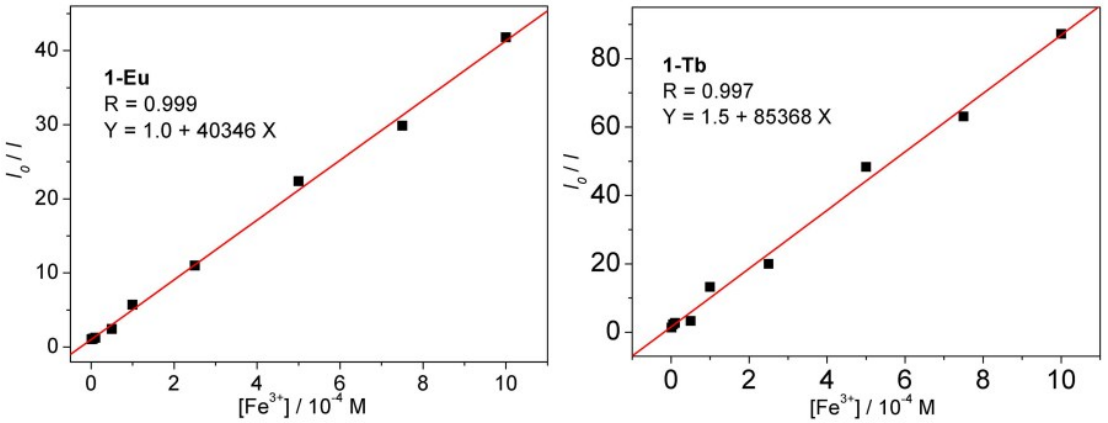

Fig. S13 The linear correlation of **1-Eu** (a) and **1-Tb** (b) for the plot of (I_0 /I) *vs* concentration of Fe^{3+} in low concentration range.

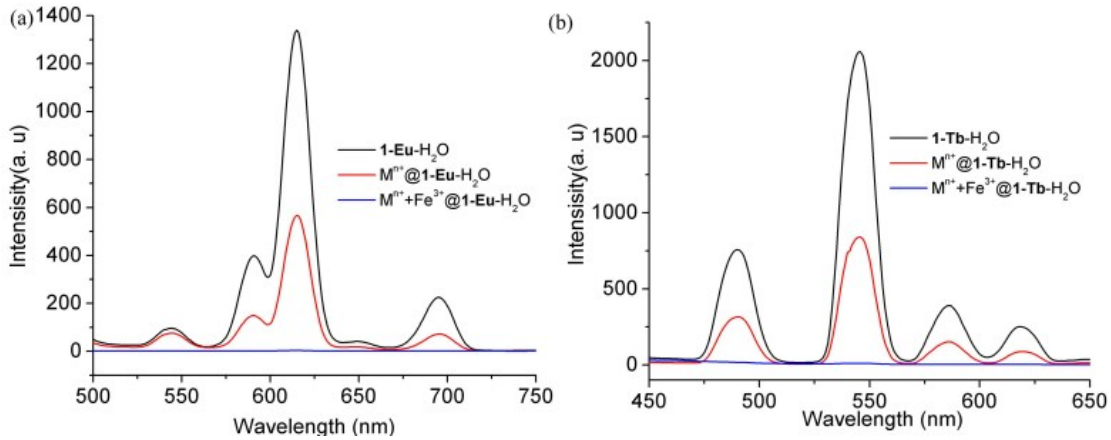

Fig. S14 Comparison of the luminescent intensity of **1-Eu**-H_2O (a) and **1-Tb**-H_2O (b) exchanged with M^{n+} ions (Pb^{2+}, Na^+, Al^{3+}, K^+, Mg^{2+}, Hg^{2+}, Zn^{2+}, Cd^{2+}, Cu^{2+}, Fe^{2+}, Ni^{2+}, Cr^{3+}, Mn^{2+}, Co^{2+}) in the absence and presence of 1 mM Fe^{3+} ion.

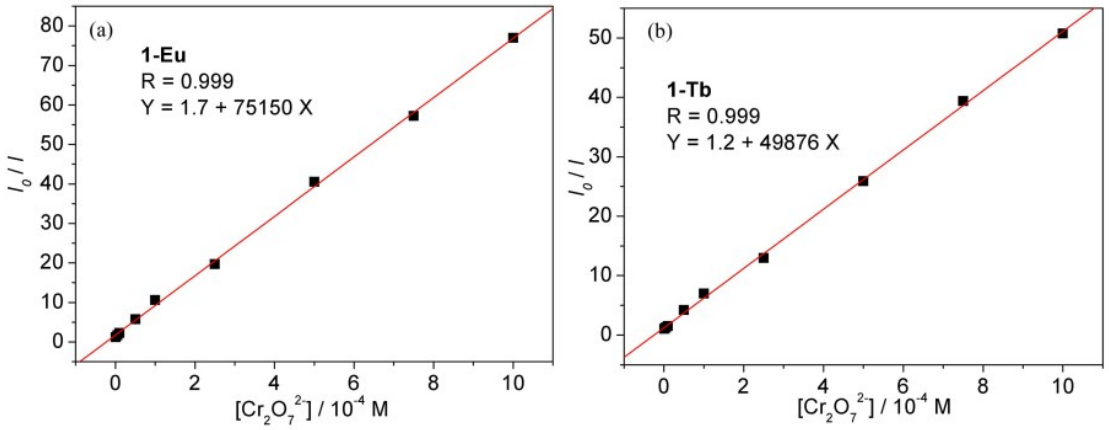

Fig. S15 The linear correlation of **1-Eu** (a) and **1-Tb** (b) for the plot of (I_0 /I) *vs* concentration of $Cr_2O_7^{2-}$ in low concentration range.

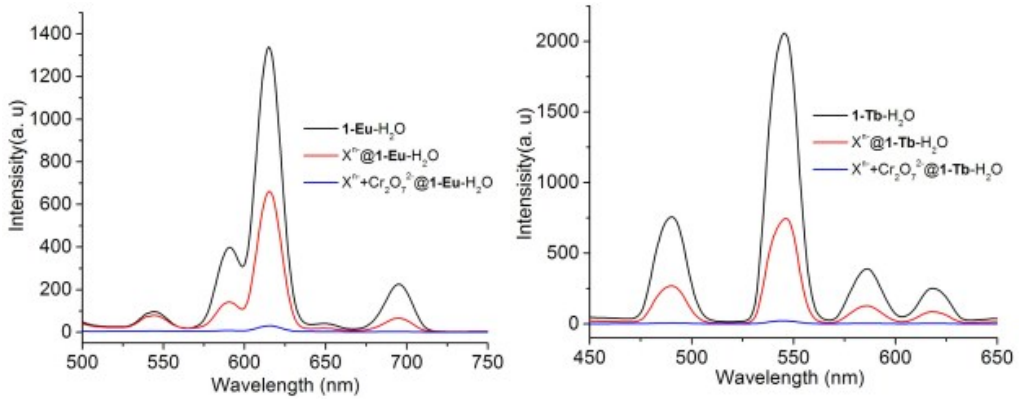

Fig. S16 Comparison of the luminescent intensity of **1-Eu-**H_2O (a) and **1-Tb-**H_2O (b) exchanged with X^{n-} ions (F^-, Cl^-, I^-, Br^-, NO_3^-, CrO_4^{2-}, ClO_3^{2-}, Ac^-, $S_2O_3^{2-}$, MnO_4^-) in the absence and presence of 1 mM $Cr_2O_7^{2-}$ ion.

References

S1 R.-C. Gao, F.-S. Guo, N.-N. Bai, Y.-L. Wu, F. Yang, J.-Y. Liang, Z.-J. Li and Y.-Y. Wang, *Inorg. Chem.,* 2016, **55**, 11323-11330.

S2 X. Guo, Y. Li, Q. Peng, Z. Duan, M. Li, M. Shao, X. He, *Polyhedron,* 2017, **133**, 238-244.

S3 L.-H. Cao, F. Shi, W.-M. Zhang, S.-Q. Zang and T. C. W. Mak, *Chem. Eur. J*., 2015, **21**, 15705-15712.

S4 S.-T. Zhang, J. Yang, H. Wu, Y.-Y. Liu and J.-F. Ma, *Chem. Eur. J*., 2015, **21**, 15806-15819.

S5 L. Li, Q. Chen, Z. Niu, X. Zhou, T. Yang and W. Huang, *J. Mater. Chem. C*, 2016, **4**, 1900-1905.

S6 S. Dang, E. Ma, Z.-M. Sun and H. Zhang, *J. Mater. Chem*., 2012, **22**, 16920-16926.

S7 G.-P. Li, G. Liu, Y.-Z. Li, L. Hou, Y.-Y. Wang and Z. Zhu, *Inorg. Chem*., 2016, **55**, 3952-3959.

S8 M. Chen, W.-M. Xu, J.-Y. Tian, H. Cui, J.-X. Zhang, C.-S. Liu and M. Du, *J. Mater. Chem. C*., 2017, **5**, 2015-2021.

S9 Z.Sun, M. Yang, Y. Ma, and L.-C. Li,*Cryst. Growth Des*., 2017, **17**, 4326-4335.